IJNAOE
©SNAK, 2014

Int. J. Nav. Archit. Ocean Eng. (2014) 6:442~458
http://dx.doi.org/10.2478/IJNAOE-2013-0191
pISSN: 2092-6782, eISSN: 2092-6790

Assessment of whipping and springing on a large container vessel

Mondher Barhoumi[1] and Gaute Storhaug[2]

[1]*Vestfold University College, Norway*
[2]*DNV GL, Maritime, Norway*

ABSTRACT: *Wave induced vibrations increase the fatigue and extreme loading, but this is normally neglected in design. The industry view on this is changing. Wave induced vibrations are often divided into springing and whipping, and their relative contribution to fatigue and extreme loading varies depending on ship design. When it comes to displacement vessels, the contribution from whipping on fatigue and extreme loading is particularly high for certain container vessels. A large modern design container vessel with high bow flare angle and high service speed has been considered. The container vessel was equipped with a hull monitoring system from a recognized supplier of HMON systems. The vessel has been operating between Asia and Europe for a few years and valuable data has been collected. Also model tests have been carried out of this vessel to investigate fatigue and extreme loading, but model tests are often limited to head seas. For the full scale measurements, the correlation between stress data and wind data has been investigated. The wave and vibration damage are shown versus heading and Beaufort strength to indicate general trends. The wind data has also been compared to North Atlantic design environment. Even though it has been shown that the encountered wind data has been much less severe than in North Atlantic, the extreme loading defined by IACS URS11 is significantly exceeded when whipping is included. If whipping may contribute to collapse, then proper seamanship may be useful in order to limit the extreme loading. The vibration damage is also observed to be high from head to beam seas, and even present in stern seas, but fatigue damage in general is low on this East Asia to Europe trade.*

KEY WORDS: Vibration; Whipping; Springing; Fatigue; Extreme loading; Container; Full scale measurements.

INTRODUCTION

There are around 100,000 merchant ships over 100 *GT* trading internationally. They transport every kind of cargo, carrying over 90% of the world trade. The average age of the ships is 22 years. Losses from a severe accident of a vessel can be high not only when it comes to fatalities, damaged ship or cargo, but also with regard to the environmental pollution (IMO, 2012). Therefore, the shipping industry is one of the most heavily regulated industries, with internationally standards related to design approval, construction and operation including inspection. The regulation of the maritime industry is mainly related to the objective of ensuring safety, security and prevention of pollution from ships. One of the increasing concerns is related to the analysis of fatigue and ultimate strength of ship structures, which is related to maintenance and repair cost as well as safety,

Corresponding author: *Gaute.Storhaug*, e-mail: *Gaute.Storhaug@dnvgl.com*

This paper has been selected from the Proceedings of PRADS 2013, reviewed by referees and modified to meet guidelines for publication in IJNAOE.

illustrated by the development of common structural rules for tankers and bulk carriers by IACS. However, there are still large uncertainties in prediction of fatigue lives, which is mainly caused by uncertainties in the actual environmental and operational profile, (Storhaug et al., 2010), as well as uncertainties associated with current calculations procedures used in design, where effects of some phenomena may be neglected at least explicitly, e.g. wave induced vibration, (Storhaug et al., 2003).

Wave-induced hull girder vibrations are normally described by the terms of springing and whipping. Springing is resonant vibrations, while whipping is transient vibrations, which increases rapidly due to wave-loads. Whipping is normally caused by an impact of loads from bottom slamming, bow flare slamming or stern slamming (or even from ice impacts, grounding and explosion which is less frequent). Full scale measurement onboard different vessel types shows that the effect of vibrations on the fatigue damage is comparable to the conventional wave loading effect. The whipping contributes to extreme loading which may also exceed the IACS URS 11 rule wave bending moment, (Moe et al., 2005; Storhaug et al., 2012).

The current paper considers an 8,600*TEU* container vessel, which is equipped with a hull monitoring system supplied by Light Structure AS (LS). The monitoring system is based on fiber optic sensors, which measure the strain in different key location of the hull structure. The system receives data from other ship systems available onboard, e.g. environmental, navigational and loading computer data. The vessel was considered in a previous research project where fatigue loading was studied based on one year of measurements. The setup and sensor location is explained in (Heggelund et al., 2011). The current paper investigates the correlation between stress data, wind heading and wind strength. The extreme loading are also assessed and compared to the stress from IACS URS11 rule wave bending (IACS, 2010).

VESSEL AND SENSORS CONSIDERED

An 8,600*TEU* container ship was built in 2009 to the DNV class notation "1A1 container carrier EO CSA-2", which implies direct hydrodynamic and structural analysis during the design phase. CSA-2 notation implies reduced risk of fatigue cracking compared to minimum industry standard for ships. This Post-Panamax vessel has been designed for 40 years target life in World Wide trade (WW). More characteristics of the ship are given in Table 1.

The vessel is equipped by a comprehensive hull monitoring system with 20 strain sensors for global and local hull response including a bow accelerometer. GPS, loading computer and wind sensor are among the sensors connected. Optical sensors give better performance and quality of the data compared to conventional strain sensors. They are smaller and more flexible in use than long-based strain sensors. Multiplexing signals are transferred with low noise and "cross talk" in fiber optic cable. More details about sensors and locations are listed in Tables 2 and 3. The system receives digitized information (wavelength of emitted light) from strain sensors and converts it to stress and corrects the stress for temperature effects. The obtained data is filtered to obtain different types of time series:

- Raw: unfiltered data (RAW).
- Dynamic: Responses with temperature/still water removed (above 0.01*Hz*) (DYN).
- Wave: wave frequency ship responses (from 0.01*Hz* to 0.3*Hz*) (WAV).
- Vibration: only vibration responses (above 0.45*Hz*) (VIB).

The times series are processed and used for several purposes like slamming event detections, warning of loading exceeding 80 and 100% of rule loading. From the time series Rainflow response spectra is also established and this is used for fatigue analysis. Statistical data are also produced and stored in statistics files for 5 minutes and 30 minutes intervals (stat5 and stat30). These statistical data have mainly been used in this paper. Some of this data is displayed on a monitor located on the bridge for decision support in bad weather.

An example of stress time series for deck sensor on port (DMP) and starboard (DMS) side amidships are shown in Fig. 1. This shows heavy whipping vibrations from bow flare impact. These whipping vibrations are superimposed on the wave loading and the contribution to the maximum stress is considerable. The small difference between the port and starboard sensors in this case suggest that the vessel encountered head seas during this short period.

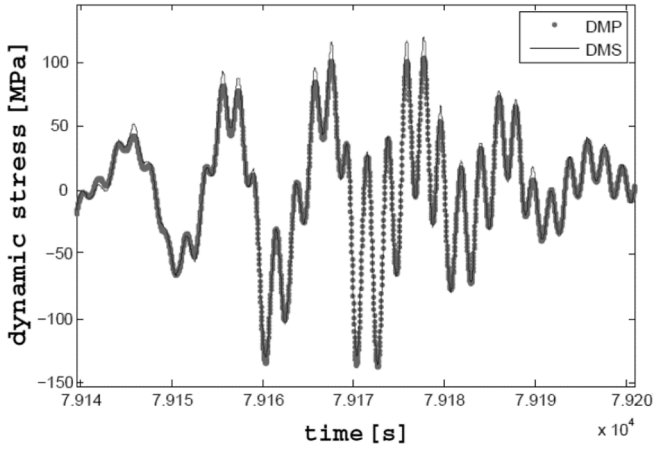

Fig. 1 Example of vibration (whipping) in the measured stress in deck amidships.

Table 1 Ship characteristics.

Main characteristics	Value
Length overall, L_{OA}	339.6*m*
Length between per. L_{PP}	322.6*m*
Rule length, L	318.41*m*
Breadth, B	45.6*m*
Depth, D	24.6*m*
Draft design, T	13*m*
Draft scantlings, T	14.5*m*
Deadweight at design, dwt.	95810*tones*
Service speed at design draft, V	28.6*knots*
Container capacity	8562*TEU*
Block coefficient, C_B	0.621 [-]
Neutral axis above base line, Zn	11.26*m*

Table 2 Sensor location and definition.

Sensor	Location	Definition
DMP/DMS	L/2	Deck midship Port/Starboard
DAP/DAS	L/4	Deck Aft Port/Starboard
DFP/DFS	3L/4	Deck Forward Port/Starboard

Table 3 Sensor characteristics.

Sensor	y [*m*]	z [*m*]	Zv [m^3]	Zh [m^3]
DMP/MS	±22.3	24.34	56.8	±104.2
DAP/AS	±21.9	24.42	50.2	±81.0
DFP/DFS	±22.1	24.35	41.3	±53.5

TRADE AND MEASUREMENT PERIOD

The data considered was collected from 3rd of June 2009 to 18th of March 2013, when the vessel was operating between Asia and Europe performing about 40 voyages from East Asia to North Europe and back. The position plot in Fig. 2 shows that the vessel was trading mainly in East Asia to Europe trade with only 15% of the time spent in North Atlantic, which is defined as north of 40° N in the Atlantic Ocean. The stored statistical data contains 390623 five minutes records, i.e. 3.7 years of effective measurements. It is observed that the amount of routing to avoid storms is close to zero and not very relevant on this main trade. This differs a lot from North Atlantic crossings.

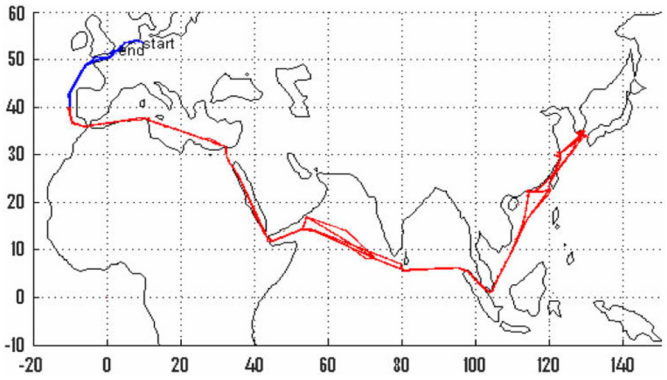

Fig. 2 Sailing area for the vessel.

FATIGUE ASSESSMENT

Fatigue analysis is based on analyzing the times series following three steps: Reversal identification, establishing the Rainflow spectra and estimating the fatigue accumulation damage. The reversals are identified when the local derivative of the time series change sign i.e. "Peak" when sign changes from positive to negative and "Valley" when it changes from negative to positive. The Rainflow counting procedures is made according to ASTM standards (ASTM, 1997). It counts the number of half cycles of a given range (bin) making spectra at regular time intervals e.g. 5 minutes or one hour. The one hour rainflow spectra are stored and used in this paper to recalculate the fatigue damage based on chosen S-N curve parameters, target fatigue lives and SCF.

The fatigue is calculated based on the rainflow spectra and Stress Concentration Factor (SCF) of 2 for the considered sensors. Thereafter, the damage summation is calculated according to Miner Palmgren rule and S-N curve for welded details in air or corrosive environment can be used (DNV, 2010). This process is made for the total stress time series, which include wave induced vibration (DYN) and this gives the total fatigue damage. Thereafter the process in made for the stress time series which is filtered to remove contribution of stresses above 0.3*Hz* (WAV), which give the wave damage. Finally, the vibration damage is the difference between the total and the wave fatigue damage. This is stored in the statistical stat5 and stat30 files as fatigue rates. Five minutes fatigue rate is defined as five minutes fatigue damage divided by the five minutes budget damage, which is depends of the target design life. The target life was set to 40 years in this case (error in reference (Heggelund et al., 2011) states 20 years, which led to wrong understanding of the maximum fatigue rates). The 5 minutes budget fatigue damage is equal to $1/(40 \times 365 \times 24 \times 12) = 2.378 \times 10^{-7}$. Similarly, the half hour fatigue rates can be calculated. Then, looking at maximum values, the 5 minutes fatigue rates are higher than 30 minutes fatigue rates where high loading events are less dominating.

However, it should be mentioned that fatigue damage is related to fatigue loading, while the real cracking may differ depending on different factors such as workmanship, SCF and coating conditions. Also the mean stress effect is neglected assuming the whole load cycles to occur in tension. This is a fair assumption since the focus is on sensors located on deck of a container ship which is a "hogging" vessel with tension in deck.

The five minutes total fatigue rates and wave fatigue rates for the port, DMP, and starboard, DMS, sensors in deck amidships are displayed in Figs. 3 and 4. The vibration contribution to the total damage is 57.4% for DMP and 54.8% for DMS. The average total fatigue rates in air are 0.18 and 0.25 for the two sensors, respectively, which correspond to fatigue lives of 222 and 158 years. The maximum 5 minutes fatigue rates are 371.7 and 373 (the maximum half hour fatigue rates are 168 and 170

for the same sensors respectively). Further, the available rainflow counting files are used to recalculate the fatigue damage from different configuration such as, corrosive S-N curve (DNV-2) (DNV, 2010) with 40 years target fatigue life, that give average fatigue rates 0.55 and 0.81 for port and starboard deck sensor, respectively, which correspond to 72 and 49 years fatigue lives. The fatigue is not regarded to be an issue if the vessel continues to operate in this East Asia to Europe trade. This may be due to the good vessel design based on CSA-2 class notation and 40 years target life, but it is also a consequence of the trade, which is less severe than World Wide trade, North Pacific or North Atlantic trade.

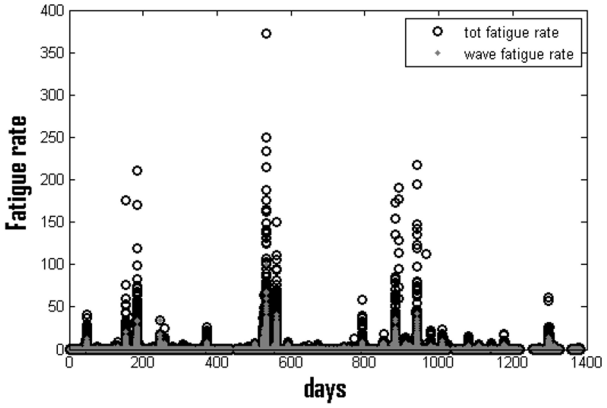

Fig. 3 Total and wave 5 minutes fatigue rates for port side deck sensor (DMP).

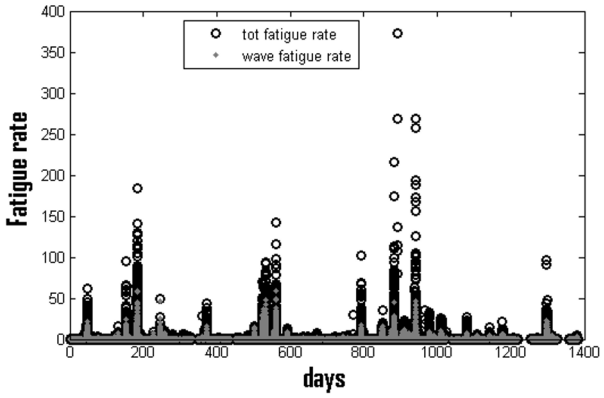

Fig. 4 Total and wave 5 minutes fatigue rates for port side deck sensor (DMS).

If we consider the port sensor in deck amidships (DMP), the time in different fatigue rate intervals and the contribution of the intervals to the total damage are displayed in Fig. 5. The fatigue rate interval of 0.01-1 refers to the time spent between 0.01 and 1. Fatigue rates are summarized for each interval and divided by the total summarized fatigue rates. 83% of the time the fatigue rates are below 0.01 and the damage in this interval is only 0.4% of the total damage. 98% of the time the fatigue rates are below the design average of 1.0, and that corresponds to 11% of the total damage. When we consider the interval of time where the fatigue rates are above 10, it consists of less than 0.5% of the total time while it accounts for 56% of the total damage. The higher fatigue rates are limited in time but critical regarding to damage contribution and that may be reduced by routing or speed reduction in order to reduce significantly the whipping contribution. For this trade routing is not relevant, so only the speed reduction is effective. A few hours of speed reduction may significantly reduce the fatigue damage, and this vessel has plenty of power to catch up in calm seas.

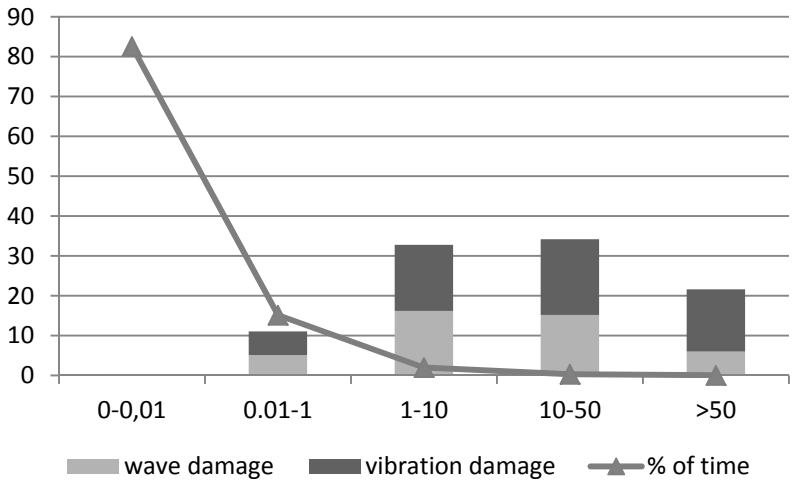

Fig. 5 % of time and % of damage in different fatigue rate intervals.

FATIGUE DAMAGE VERSUS WIND CONDITIONS

The system receives also data from other ship systems, such as the GPS and the wind sensor. The collected wind data give the wind speed and direction relative to the ship every 5minutes. It should be noted that the wind sensor has not been always effective during the period before 21st of December 2010, and due to these unreliable results the wind records before this data has been omitted in the following analysis. The remaining period covers 2.3 years of data. Before using the wind data in the analysis, it has to be corrected for the forward speed of the vessel as well as its relative heading. This is shown in Eqs. (1) and (2).

$$\beta_{real} = \tan^{-1} \frac{V_m * \sin(\beta_m)}{V_m * \cos(\beta_m) - V} \tag{1}$$

$$V_{real} = \frac{V_m * \sin(\beta_m)}{\sin(\beta_{real})} \tag{2}$$

where, β_{real} is the corrected wind direction relative to the ship and V_{real} is the real wind speed. β_m and V_m are the measured wind direction and speed respectively, and V is the vessel speed.

The wind sensor is located about 43.5*m* above the sea surface. The wind speed has to be corrected down to 10*m* above the sea surface which is the reference for the Beaufort scale. This is shown in Eq. (3).

$$V_{10} = V_{real} * (\frac{10}{h})^{1/7} \tag{3}$$

V_{10} is the wind speed at 10*m* above the sea surface while h is the sensor height.

The wind speed is converted to Beaufort scale and the probability distribution of the wind as function of Beaufort number is shown in Fig. 6. Only measurements when the vessel speed was above 3 *knots* are considered. The records when the vessel is "in port area" are neglected in plotting the probability distribution. Comparing to Argoss data in open sea for the North Atlantic trade, the measured wind is much less severe. Bn number 3 is most frequent. Bn of 5 is most frequent from Argoss, which have much higher probabilities for higher Bn. This is as expected for this trade. East Asia to Europe is much less severe than North Atlantic.

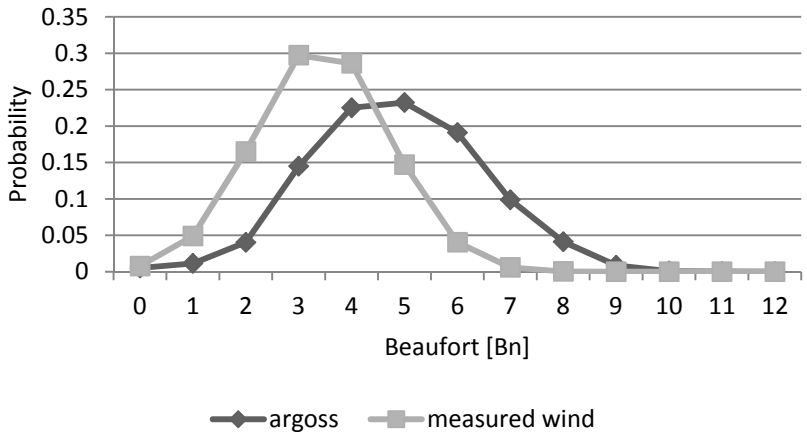

Fig. 6 Measured wind strength distribution versus argoss.

The average five minutes fatigue rates and the vibration contribution to fatigue damage as function of Beaufort strength are displayed in Fig. 7. The vibration contribution increase with the increase of the wind strength, from 34% for Bn = 1 to 73% for Bn = 9. The average five minutes fatigue damage increase with the wind and it exceeds the budget fatigue damage for Bn = 7

and above. It should be noted that the average fatigue rates are low as a result of all headings being included. This also affects the vibration contribution, which is expected low in e.g. beam seas and wind conditions.

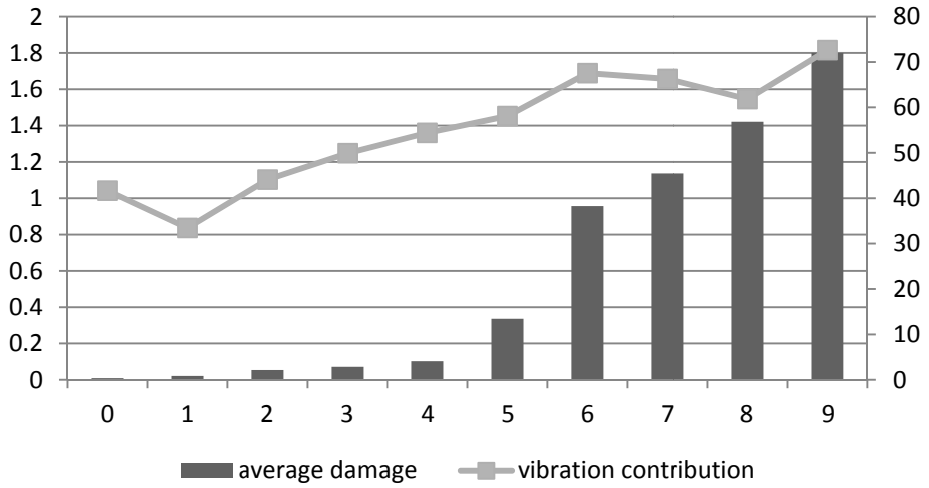

Fig. 7 Average 5 minutes fatigue rates and vibration contribution as function of Bn.

The relative wind direction can be divided into 6 sectors. Head wind is defined as $0 \pm 30°$, which refer to sector 1, while stern wind is $180 \pm 30°$, which refers to sector 6. The other sectors have 30° steps and port and starboard observations are merged, see Fig. 8.

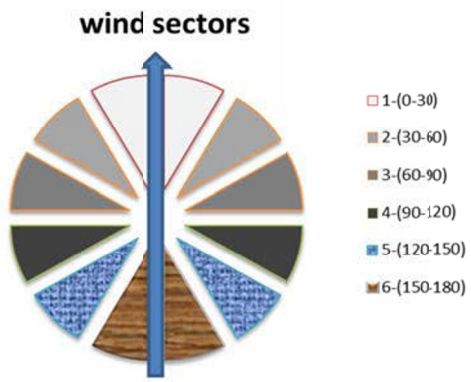

Fig. 8 Wind sectors.

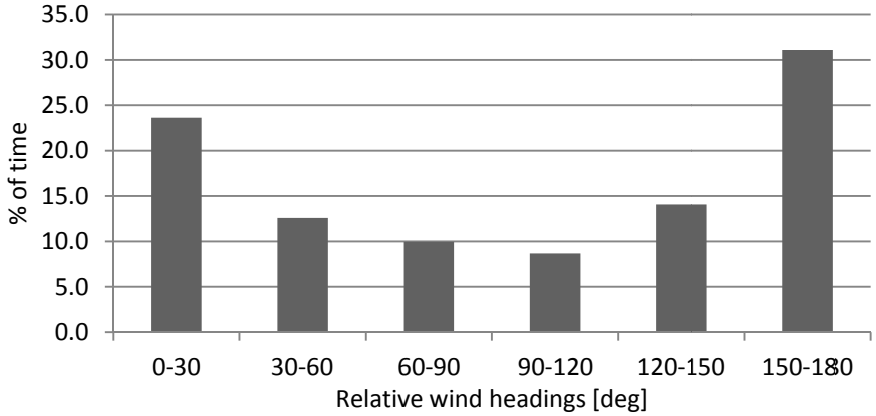

Fig. 9 Relative wind heading profile.

The relative wind headings distribution is displayed in Fig. 9, which shows that the stern and head winds are dominating with 31% and 24% encounter probability, respectively. The true wind (relative to north) distribution, illustrated in the Fig. 10, shows that the wind is quite evenly distributed between the 6 sectors. Northern (wind coming from northern) and northeastern winds are, however, slightly prevailing. This is expected for the Northern Indian Ocean where the ship spends a relatively high part of the time.

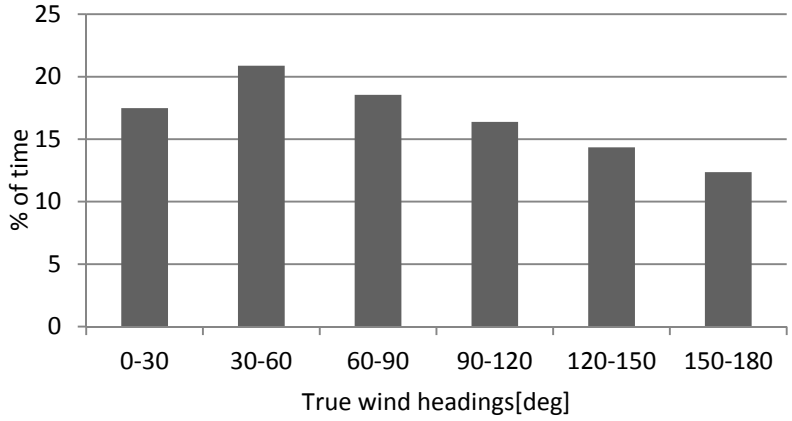

Fig. 10 True wind heading profile.

Figs. 11 and 12 show the percent of damage and vibration damage contribution as function of wind headings, for both sensors DMP and DMS. Head and bow quartering winds are much more important than other headings with 29.5% and 28.3% contribution, respectively, for the DMP sensor. While beam winds (sector 4) have the lowest importance with 4.4% for DMP sensor. It is clear that the vibration contribution decays from bow quartering, 66%, to stern seas, 44%. The DMP and DMS shows consistent results, but the differences can be explained by the heading profile not being completely symmetric. Another significant observation is that vibration is clearly present also in stern winds, which also have been observed on other container vessels (Storhaug, 2012).

Tables 4 and 5 show the fatigue damage versus wind headings. Based on the average fatigue rates and the probability for each heading, the wind headings are rated from the most critical regarding to fatigue damage to the least critical. Results are identical for both sensors DMP and DMS, and sectors 2 and 3 are considered the worst headings. The reason for head wind not producing worse results could be because the encountered sea states can be considered relatively small for this long vessel (340 m L_{OA}), so it is quartering seas that gives more significant wave bending moment as the wave length then appears longer. This will similarly affect stern wind heading. Further, in stern seas also the frequency of encounter is reduced compared to head seas, which results in fewer fatigue cycles per hour and thereby also lower fatigue damage in general.

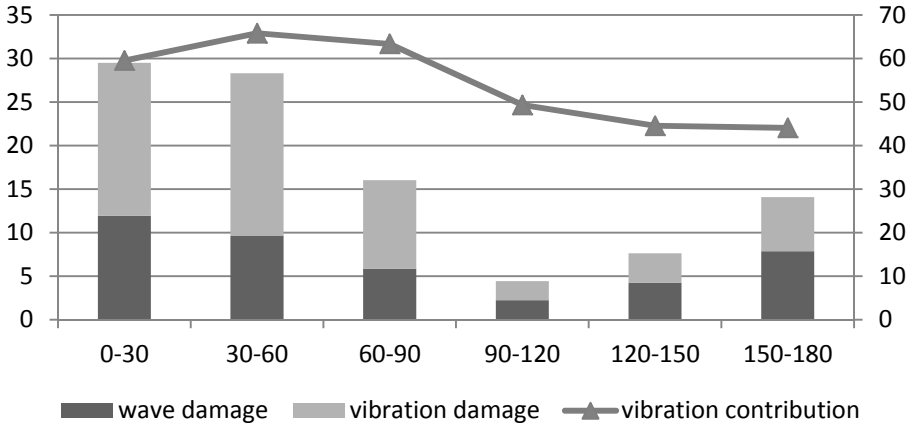

Fig. 11 % of damage (left) and relative wave/vibration damage (right) versus wind sectors (DMP).

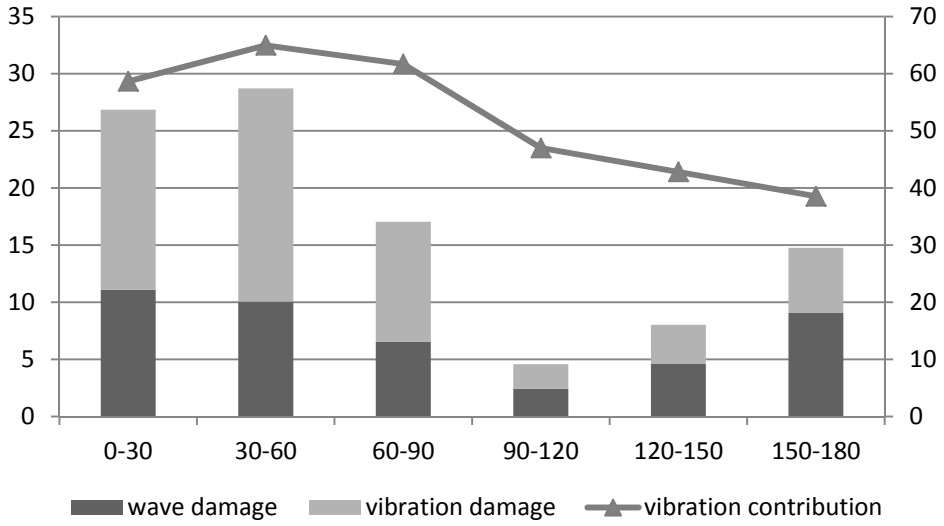

Fig. 12 % of damage (left) and relative wave/vibration damage (right) versus wind sectors (DMS).

Table 4 Fatigue damage versus wind heading (DMP).

Wind sectors	% time	% damage	Average damage	Rating
0-30	23.6	29.5	0.17	3
30-60	12.6	28.3	0.31	1
60-90	10.0	16.1	0.22	2
90-120	8.7	4.43	0.07	5
120-150	14.1	7.64	0.07	4
150-180	31.1	14.1	0.06	6

Table 5 Fatigue damage versus wind heading (DMS).

Heading	% time	% damage	Average damage	Rating
0-30	23.6	26.85	0.24	3
30-60	12.6	28.72	0.49	1
60-90	10.0	17.05	0.38	2
90-120	8.7	4.59	0.11	5
120-150	14.1	8.03	0.12	4
150-180	31.1	14.76	0.10	6

Considering the sector 2, Figs. 13 and 14 show the corresponding total damage distribution, relative vibration contribution, average five minutes damage and average speed for each Bn number. It should be noted that Bn 0 and Bn 7 has few observations. The average damage increases with increasing Bn, and it exceeds significantly the design budget damage for Bn 6 and 7. The vibration contribution increases from 30% for Bn 1 to about 73% for Bn 7. Bn = 6 is the most contributing to fatigue damage with about 38%. The maximum average speed is about 17 *knots* and decrease slightly after Bn 2.

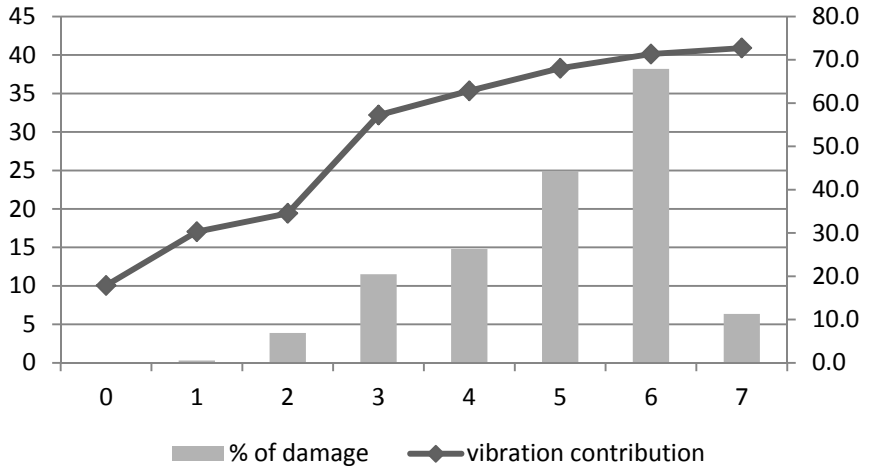

Fig. 13 % of damage and vibration contribution versus Bn in sector 2 (DMP).

Bn	0	1	2	3	4	5	6	7	8	9
Obs.	31	1024	4092	5036	3937	1912	840	104	0	0

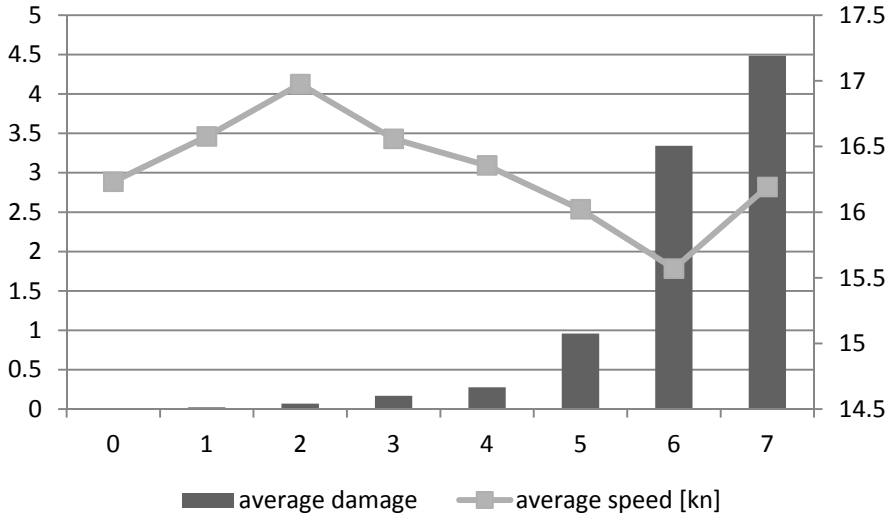

Fig. 14 Average damage and average speed versus Bn in sector 2 (DMP).

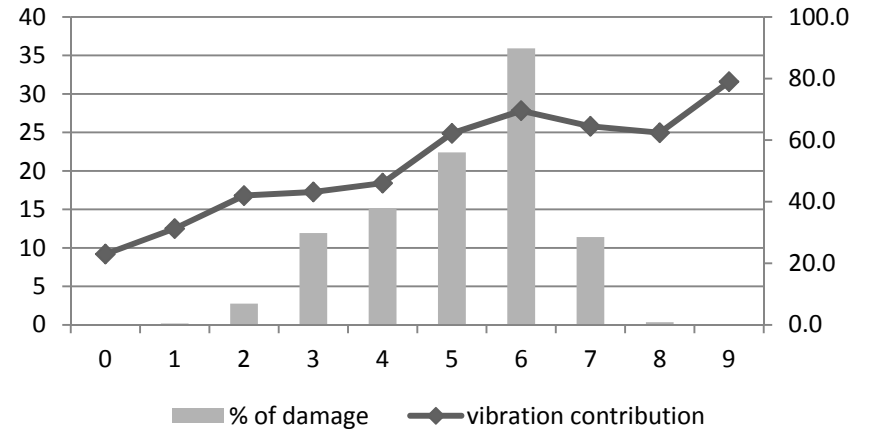

Fig. 15 % of damage and vibration contribution versus Bn in sector 1 (DMP).

For head wind (sector 1), the same diagrams are shown in Figs. 15 and 16. There are few observations for high Bn 8 and 9 as well as Bn 0. The average damage has tendency to increase with increasing Bn to about 1.3 for Bn 7, while it decays again for Bn 8 and 9 (only 3 observation for Bn 9). It may happen that Bn 9 is related to the vessel being close to shore and that the waves actually are small due to short fetch even though the wind is strong. The vessel speed decreases with increasing Bn, and significant speed reduction is observed at Bn 8 and 9. This may also affect the vibration contribution and average fatigue damage. Bn 6 contributes most to fatigue damage with 36%. The vibration contribution to fatigue damage increases with Bn from 32% for Bn 1 to 79% for Bn 9. The results for sector 1 are in fair agreement with sector 2.

Bn	0	1	2	3	4	5	6	7	8	9
Obs.	33	1184	4413	8423	10961	6809	2631	731	40	3

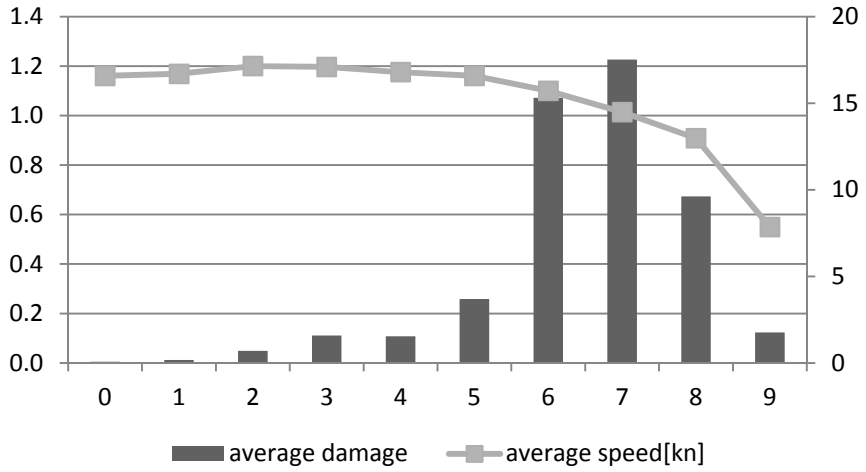

Fig. 16 Average damage and average speed versus Bn in sector 1 (DMP).

For stern seas (sector 6), the total damage and vibration contribution versus Bn are displayed in Fig. 17 and the average 5 minutes fatigue rates with the average speed as function of Bn are displayed in Fig. 18. The average damage is quite low even for Bn up to 7, while significant for Bn 8 and 9, which has few observations. , The vibration contribution does not show a clear trend and varies between 26% for Bn 5 to 70% for Bn 9. The average speed increases with increasing Bn as expected and observed on other ships (Storhaug, 2012). Bn 4 contributes most to the fatigue damage for stern seas in sector 6. The results are quite different from sector 1 and 2, but vibration effects are still present and significant in stern wind.

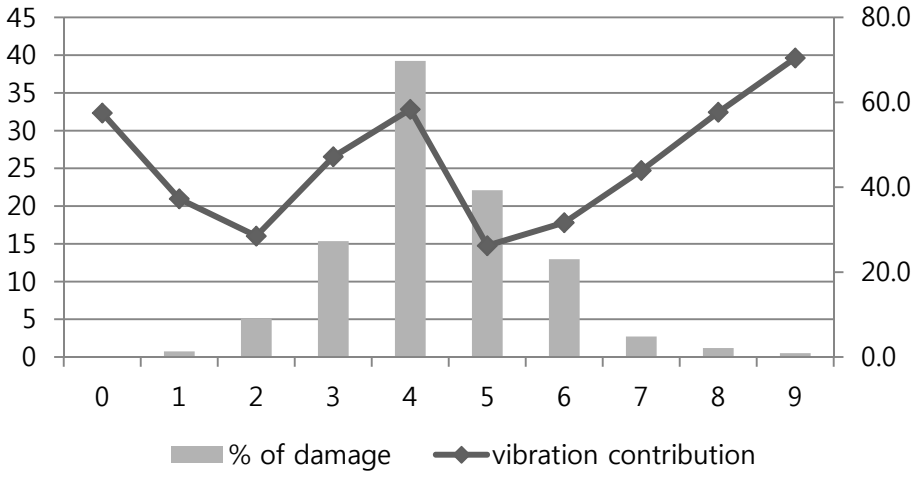

Fig. 17 % of damage and vibration contribution versus Bn in sector 6 (DMP).

Bn	0	1	2	3	4	5	6	7	8	9
Obs.	356	1449	6345	15247	20614	9377	3056	557	51	9

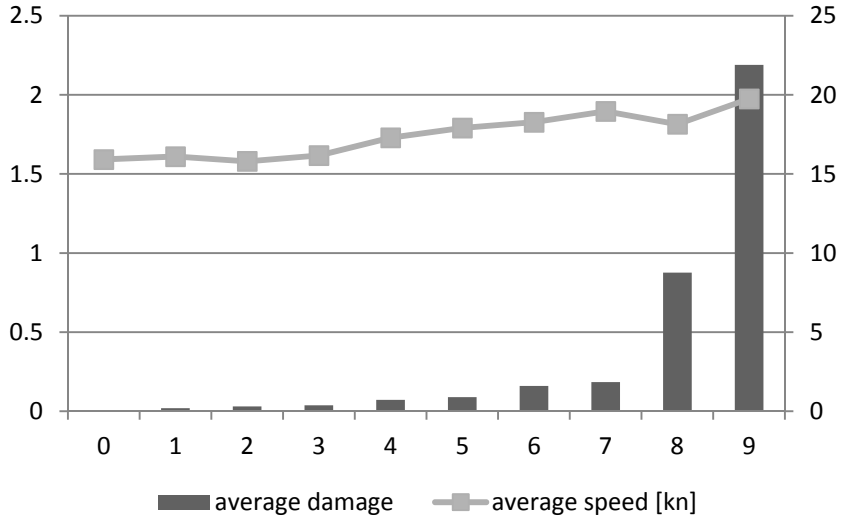

Fig. 18 Average damage and average speed versus Bn in sector 6 (DMP).

A voluntary speed reduction in harsh environment may be effective to reduce the fatigue damage and in particular the vibration contribution in head and bow quartering seas. In Fig. 19, the fatigue rates for starboard deck sensor DMS are shown together with ship speed, wind relative heading and Beaufort strength for the day 30th December 2011. A relative scale is used for better comparison. The vessel was sailing in the Strait of Sicily, north of Tunisia (one of the severest areas in the Mediterranean Sea in December). The period with high fatigue rates lasts for about ½ a day. The average 5 minutes fatigue rate during this day is 29, meaning that 29 days of budget is spent. The speed is reduced from about 21 to 13 *knots*. Hence, the fatigue rates were reduced significantly. If the speed were reduced 9 hours earlier, the average fatigue rates would have been reduced further during this day and possibly the fatigue damage from this day could have been reduced down to 1/3. For this vessel it is not critical, but encountering such storms frequently, e.g. once on each crossing in a North Atlantic trade would result in undesirable low fatigue life.

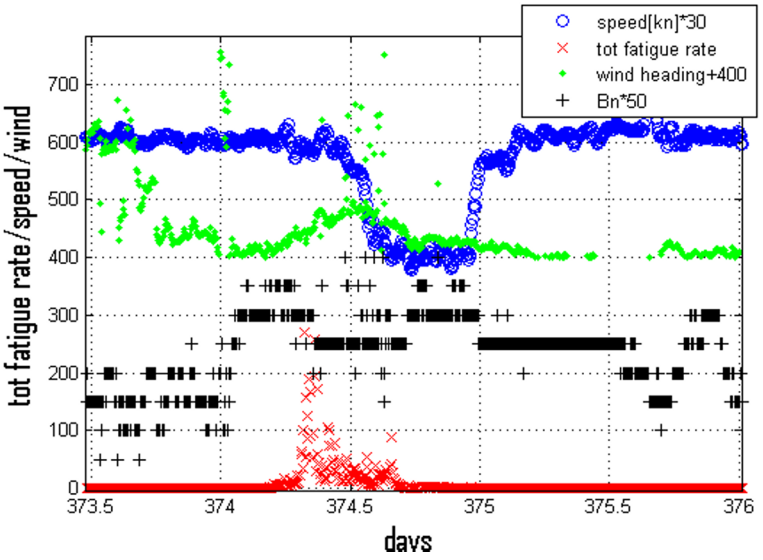

Fig. 19 Fatigue rates (DMS), vessel speed, wind heading, Bn, 30th December 2011.

EXTREME LOADING

For the stress level in deck amidships, the dominating contribution comes from the vertical bending moment, especially at high stress levels. Other components of the stress are axial force, horizontal bending moment and axial warping stresses. In addition, the still water bending will contributes to the overall loading. During the measurement period, the minimum (sagging) and maximum (hogging) dynamic values are determined for each 5 minutes. This is done for both the total signal that included whipping and also for the wave frequency signal, and the results are illustrated in Figs. 20 and 21 for sensors DMP and DMS, respectively. The stress from the rules wave bending moment from IACS-URS11 is 103*MPa* in hogging and 127*MPa* in sagging (an inaccuracy in reference (Heggelund et al., 2011) states 106*MPa* in hogging and 131*MPa* in sagging, which may differ depending on how the section modulus is estimated and which drawing revision that has been used). In all the encountered storms the dynamic stress of the wave response signal has been below the IACS rule stress, while this level has been exceeded by the whipping contribution several times both in hogging and sagging. For the DMP sensor the stress was recorded above the rule bending stress in 4 encountered storms, while for the starboard sensor DMS this level has been exceeded in 3 storms. In general, the maximum sagging and maximum hogging are relatively symmetric and they are quite similar for both deck sensors amidships, but port side sensor show higher extreme values than starboard sensor. This may be caused by not pure head sea conditions where other components also contribute. A slight heel may also cause this difference in stress between starboard and port deck stresses. It is observed that the hogging (positive) values are more frequently exceeded than the sagging values, also because the sagging rule values are higher.

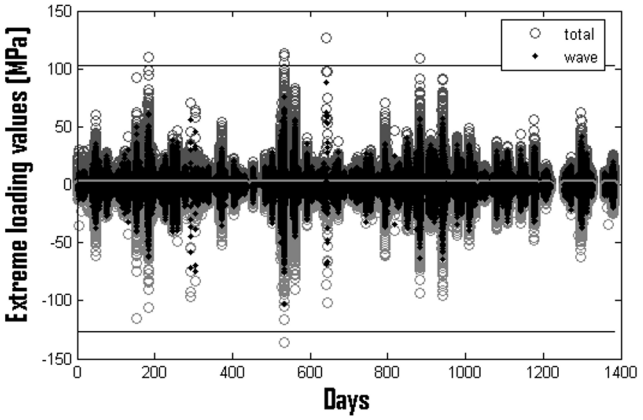

Fig. 20 The maximum 5 minutes hogging (positive) and sagging stress with and without whipping, DMP.

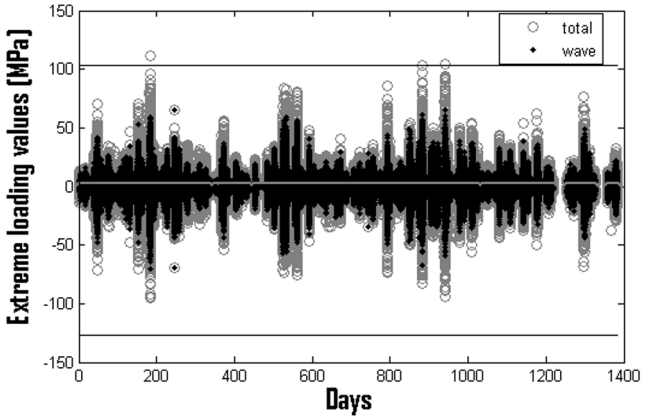

Fig. 21 The maximum 5 minutes hogging (positive) and sagging stress with and without whipping, DMS.

The highest extreme values with whipping and the highest extreme values without whipping for all the global deck sensors are shown in Table 6 based on stress values in *MPa*. The ratio of those stresses defines the amplification factor due to whipping.

The highest extreme values for the total and wave response may however occur in different storms, in the way that extreme loading from wave without whipping may come from a swell like head or stern sea condition while extreme loading when the whipping is significant may come from a steep moderate sea combined with high forward speed in head or bow quartering sea states. The amplification factors are high and in some cases the dynamic stress is doubled due to whipping. This may easily happen for this vessel with large bow flare and capable of maintaining high speed in harsh sea states. Without proper seamanship and voluntary speed reduction in moderate head sea storms it is possible that the stress level would have been even higher. The extreme values that exceed the IACS rule value are indicated in bold. It occurs in both sagging and hogging for the aft and the midship section, while the forward quarter length section is well below rule values. This is displayed more clearly in Fig. 22, where the maximum extreme loading dynamic stress with and without whipping are divided by the IACS rule wave bending stress. The excess is 48% in hogging aft and 23% in hogging amidships while more than 20% below the rule values in the fore ship. Also maximum sagging is above IACS value by 7% amidships and similarly in the aft ship. It is clear that the hogging values are relatively high, also considering that these will be combined with a still water hogging moment in an ultimate capacity check of the hull girder.

Table 6 Maximum sagging and hogging stress with and without whipping and the IACS wave bending stress rule.

Location		L/4		L/2		3L/4	
Sensor		DAP	DAS	DMP	DMS	DFP	DFS
Hogging	Total	**108**	**94.4**	**126.6**	**111.8**	70.7	60.2
	wave	52.9	49.9	88.6	65.4	46.8	36.6
	IACS	73.0	73.0	103.2	103.2	101.4	101.4
	$F_{amplification}$	2.1	1.9	1.4	1.7	1.5	1.6
Sagging	Total	**-99**	**-116**	**-136.4**	-95.5	-96.4	-99.6
	Wave	-59	-59	-102	-70.5	-59.4	-51.3
	IACS	-90	-90	-127.1	-127	-125	-125
	$F_{amplification}$	1.7	2.0	1.3	1.4	1.6	1.9

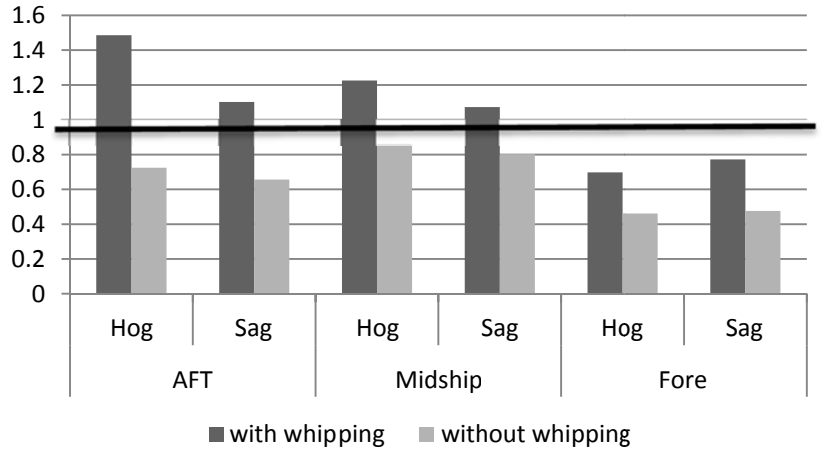

Fig. 22 The Measured stress versus IACS Rule stress from port side sensors.

The maximum sagging (min_dyn) and hogging (max_dyn) extreme stress from DMP sensor as function of Bn strength and as function of wind headings are illustrated in Figs. 23 and 24, respectively. The extreme loadings are higher in head and stern seas and decrease in beam seas. The maximum sagging and hogging is actually encountered in stern seas. It should be noted

that the wind sensor was not reliable/operational in some of the worst storms, so the worst values are not included in Figs. 23 and 24. The maximum values also occurred in moderate Bn, suggesting that this are not real wind generated storms but either swell, which are not steep sea states, or moderate sea conditions. The vessel has simply not encountered any really harsh storms yet, but the worst values refer to a sea state of about 5.5*m* significant wave height, measured by the wave radar onboard. In a North Atlantic trade higher values should be expected. In Fig 23 there is no clear correlation between maximum dynamic stress and Bn strength. The maximum dynamic stress of 126.6*MPa* (hogging) has been recorded at the wind condition of Bn 4 and stern wind combined with a forward speed of 20 *knots*. While for Bn 5 combined with higher forward speed of 21 *knots*, the maximum dynamic stress was 85*MPa* (sagging) in bow quartering. In any case the wind is moderate at it is likely that swell may be the reason for some of these high loadings. It is expected that wave parameters like significant wave height and peak period as well as heading will correlate better with extreme loadings than wind.

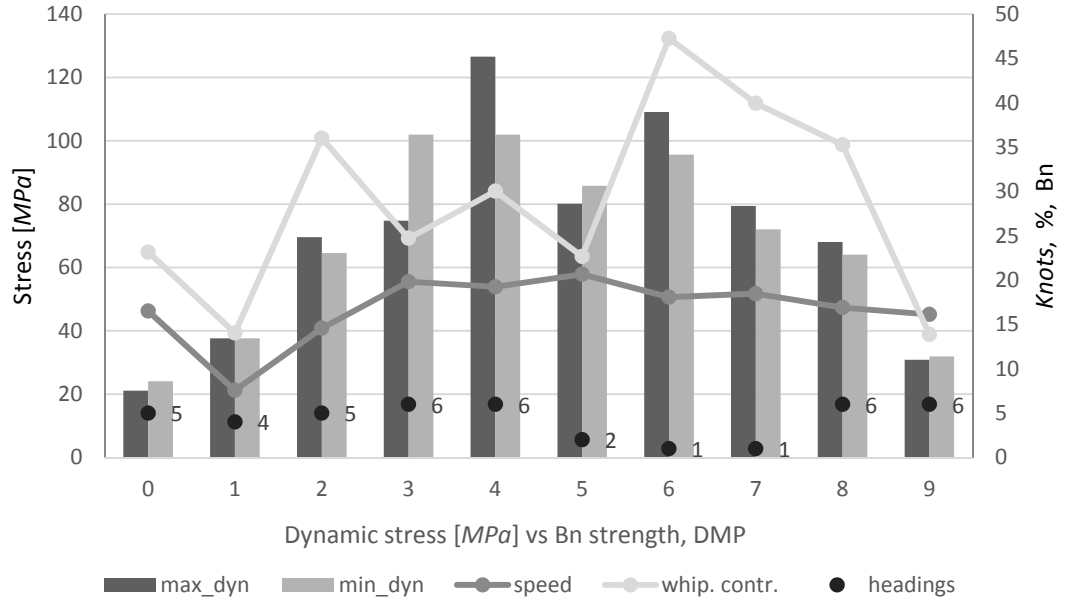

Fig. 23 The Extreme dynamic loading versus wind strength for DMP.

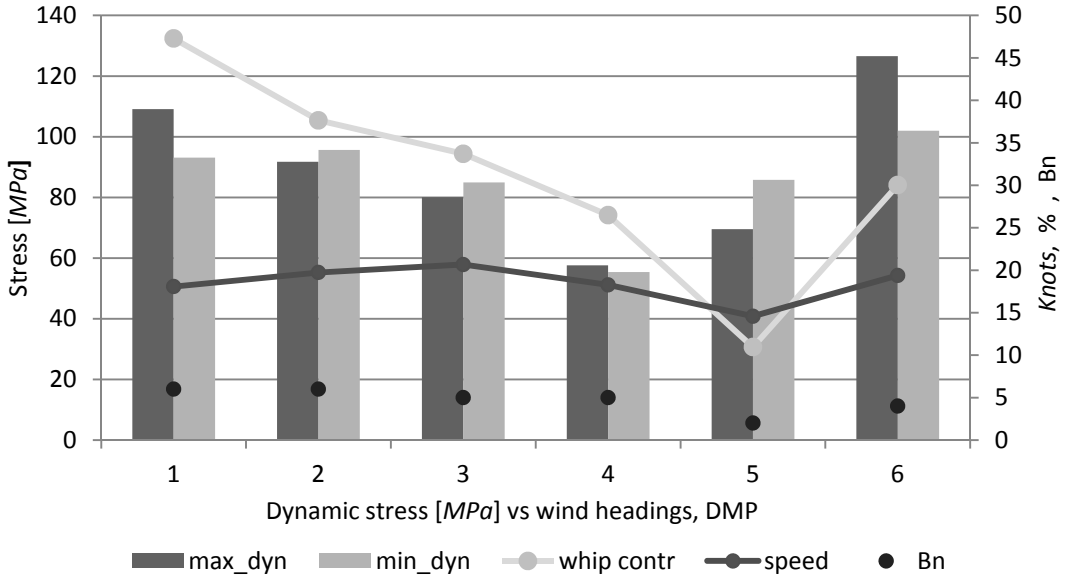

Fig. 24 The Extreme dynamic loading versus wind headings for DMP.

CONCLUSIONS

An 8,600*TEU* container vessel has been investigated. It has been sailing in East Asia to Europe trade. Measurements have been collected from about 4 year's period. The estimated fatigue life from the measurements is 49 years based on a corrosive SN-curve and a stress concentration factor of 2. Even though the vibration contributes to about 57% of the fatigue damage amidships, fatigue is not regarded as an issue for this trade and vessel. The vessel has encountered low wind strength conditions compared to the North Atlantic. The maximum fatigue rates even in this "calm" trade has been record high and exceeds what has been experienced as maximum fatigue rates on Panamax container vessel in North Atlantic. It can therefore not be concluded that fatigue for this vessel would not have been an issue if this vessel is trading regularly in North Atlantic trade. This trade is not so relevant for this Post Panamax size today, but may become relevant in the future.

The measured wind profile suggest that Bn (Beaufort strength) of 3 is most frequent. The true heading profile suggest prevailing wind conditions from northern and north eastern direction, while head and stern seas dominates slightly the encountered wind direction on this trade. The position plot confirms that routing to avoid storms is not carried out even though voluntary speed reduction is observed. From the fatigue assessment it is clear that most of the fatigue damage comes from head to beam seas, while beam to stern seas give minor contribution. Bow quartering is worst possibly due to the wave being effectively longer compared to this large vessel. The relative vibration contribution is large and decays from head to stern seas, but it is still significant in stern seas. Considering individual headings, head and bow quartering seas show an increasing average fatigue rate with increasing Bn. Also the vibration damage contribution increases with Bn, and Bn of 6 contributes to most of the damage. The speed also tends to be reduced for increasing Bn. In stern seas Bn 4 contributes most and the speed increases with Bn. Even though the average damage tends to increase with Bn the trend relative vibration contribution is not clear. In general the trend is in fair agreement with Panamax vessels in the North Atlantic.

The whipping contributes significantly to increase the dynamic extreme stresses in deck, doubling the dynamic extreme stress in both hogging and sagging at aft quarter length. The effect of whipping can also be considerable amidships and at forward quarter length. With whipping the total dynamic stress exceeds the IACS rule in both sagging and hogging at aft quarter length and amidships. The exceedance has been up to 48% in hogging at aft quarter length, corresponding to where MSC Napoli broke in two. In the forward quarter length the IACS rule stress has not been exceeded, and the wave frequency stress has not in any cases exceeded the IACS rule stress. The vessel has not encountered any real severe storms yet, only up to 5.5*m* significant wave height for the highest measured stress so far, but the extreme measured values have been encountered in moderate/small storms but at high speed. All of this agrees fairly well with observations of the same vessel in model tests. The extreme loading values do not correlate well with the wind strength since it appears that swell may affect the measured extreme stress in the various headings. For this correlation it would have been better to use wave heights and wave periods, but for the fatigue the wind sensor tends to provide useful data.

Given that the contribution of whipping is high both in fatigue and extreme loading, good seamanship is considered useful even though routing appears less relevant in this trade. This seamanship may become more significant on these large container vessels with high bow flare angle and capable of maintaining high speed in harsh head sea storms simply because the tall superstructure will make it uncomfortable on the bridge when exposed to high acceleration levels in all three directions due to high whipping events. This factor may be important in development of ship design rules when whipping should be included explicitly on container vessels. Neglecting realistic assumptions in sea states, routing and seamanship may result in too conservative guidelines.

REFERENCES

ASTM, 1997. *Standard practices for cycle counting in fatigue analysis, Annual Book of ASTM Standards. Vol 03.01, designation E1049-85*. USA: ASTM.

DNV, 2010. *Fatigue Assessment of Ship structures . DNV Classification Note No. 30.7*. Oslo: DNV.

Heggelund, S.E., Storhaug, G. and Choi, B.K., 2011. Full scale measurements of fatigue and extreme loading including whipping on an 8,600*TEU* post panamax container vessel in Asia to Europe trade. *OMAE, ASME,* Rotterdam, Holland, 19-24 June 2011.

IACS, 2010. *Longitudinal strength standard, Unified Requirements concerning strength of ships S11, Rev. 7. 2010*. London: IACS Limited.

IMO, 2012. *International shipping facts and figures-information resources on trade, safety, security, environment.* London: IMO.

Moe, E., Holtsmark, G. and Storhaug, G., 2005. Full scale measurements of the wave induced hull girder vibrations of an ore carrier trading in the North Atlantic. *RINA, International Conference, Design and Operation of bulk carriers*, London, UK, 18-19 October 2005, pp.57-85.

Storhaug, G., 2012. The effect of heading on springing and whipping induced fatigue damage measured on container vessels. *The 6th International Conference on Hydroelasticity in Marine Technology*. Tokyo, Japan, 19-21 September 2012, pp.299-310.

Storhaug, G., Choi, B.K., Moan, T. and Hermundstad, O.A., 2010. Consequence of whipping and springing on fatigue for a 8,600*TEU* container vessel in different trades based on model tests. *PRADS2010.* Rio de Janeiro, Brazil, 19-24 September 2010, pp.1210-1223.

Storhaug, G., Pettersen, T., Oma, N. and Blomberg, B., 2012. The effect of wave induced vibrations on fatigue loading and the safety margin against collapse on tow LNG vessels. *The 6th International Conference on Hydroelasticity in Marine Technology*, Tokyo, Japan, 19-21 September 2012, pp.355-366.

Storhaug, G., Vidic-Perunovic, J., Rudinger, F., Holtsmark, G., Helmers, J.B. and Gu, X., 2003. Springing/whipping response of a large ocean going vessel - A comparison between numerical simulations and full scale measurements. *3rd international conference on Hydroelasticity in Marine Technology*. Oxford, UK, 15-17 September 2003, pp.117-131.